

State-of-the-Art Review

Placental lakes vs lacunae: spot the differences

E. JAUNIAUX^{1*} , N. ZOSMER²,
F. D'ANTONIO³ and A. M. HUSSEIN⁴

¹EGA Institute for Women's Health, Faculty of Population Health Sciences, University College London (UCL), London, UK; ²Fetal Medicine Research Institute, Harris Birthright Research Centre, King's College Hospital, London, UK; ³Center for Fetal Care and High-Risk Pregnancy, Department of Obstetrics and Gynecology, University of Chieti, Italy; ⁴Department of Obstetrics and Gynecology, University of Cairo, Cairo, Egypt

*Correspondence. (e-mail: e.jauniaux@ucl.ac.uk)

ABSTRACT

*Sonographic sonolucencies are anechoic areas surrounded by tissue of normal echogenicity, commonly found in the placental parenchyma during the second and third trimesters of pregnancy. The ultrasound appearance of lakes and lacunae derives from the low echogenicity of villous-free areas within the placental parenchyma, filled with maternal blood of varying velocities. In normal placentation, lakes usually start appearing as soon as maternal blood begins to flow freely within the intervillous space at the end of the first trimester, whereas, in accreta placentation, lacunae develop progressively during the second trimester. Larger lakes are found mainly in areas of lower villous density under the fetal plate or in the marginal areas, but can also be found in the center of a lobule above the entry of a spiral artery. Lakes of variable size, position and shape are of no clinical significance, except if they transform into echogenic cystic lesions, which have been associated with poor fetal growth and placental malperfusion. Lacunae are formed by the distortion of one or more placental lobules developing inside a uterine scar, resulting from high-volume, high-velocity flows from the radial/arcuate arteries, and are associated with a high probability of placenta accreta spectrum at birth. They often present with ultrasound signs of uterine remodeling following scarring. Lakes and lacunae can coexist within the same placenta and both will change in size and shape as pregnancy advances. Better understanding of the etiopathology of placental sonolucent spaces and associated morphological changes is necessary to identify patients at risk of subsequent complications during pregnancy and/or at delivery. © 2023 The Authors. *Ultrasound in Obstetrics & Gynecology* published by John Wiley & Sons Ltd on behalf of International Society of Ultrasound in Obstetrics and Gynecology.*

INTRODUCTION

Sonographic sonolucencies or translucencies are anechoic areas surrounded by tissue of normal echogenicity. First described using B-mode ultrasonography in adult organs such as the gallbladder¹, the term 'sonolucencies' was used increasingly in the 1970s to describe placental lesions, such as subchorionic thrombosis and hematomas and cystic changes associated with gestational trophoblastic disorders². The development of high-resolution grayscale imaging allowed for more accurate evaluation of different placental lesions³. The ultrasound appearance of lakes and lacunae derives from the low echogenicity of villous-free areas within the placental parenchyma, filled with maternal blood of varying velocities. With the advent of color Doppler imaging (CDI), it became possible to link the development of these lesions to changes in the uteroplacental and fetal circulation⁴. Terms such as 'placental lake' and 'placental lacuna' started to be used more often to describe focal placental anatomical changes associated with specific placenta-related disorders of pregnancy. In the present review, we illustrate the ultrasound features and etiopathology of placental lakes and lacunae, with the aim of better understanding the development of these lesions in different placenta-related pregnancy complications and facilitating their differential diagnosis on ultrasound.

PLACENTAL LAKES

Genesis

In normal human pregnancy, the intervillous circulation within the definitive placenta is established fully by the end of the first trimester^{5–7}. Up to around 11–12 weeks of gestation, the tips of the spiral arteries are plugged by extravillous trophoblastic cells and the fetal nutritional pathway is described as histiotrophic, involving the decidual glands, chorionic cavity and secondary yolk sac⁸.

Moving echoes detected on Doppler ultrasound and indicative of significant flow become detectable in the intervillous space at the start of the second trimester of pregnancy^{5,9}. Jets of maternal blood emerging from the spiral arteries create a villous-free cavity in the center of each lobule, which is often too small to visualize on ultrasound. This is associated with the appearance of small sonolucent spaces in the center of placental cotyledons and in areas of lower villous density, mainly under the chorionic plate or in the marginal areas (Figure 1). As pregnancy advances and blood-flow volume increases in the uterine circulation, placental lakes become increasingly visible on ultrasound imaging^{3,10}. The diameter of spiral arteries may vary slightly depending on the size of the basal plate and location of

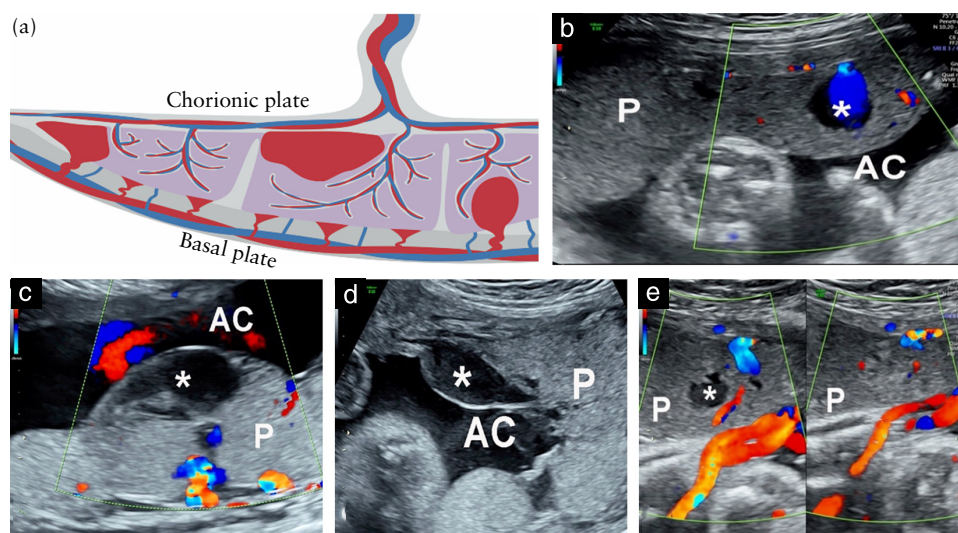


Figure 1 (a) Diagram showing common locations of placental lakes (marginal, subchorionic and centrolobular). (b–e) Longitudinal transabdominal ultrasound images of placenta (P) in uncomplicated pregnancies, showing: (b) centrolobular lake (*) at 32 weeks; (c) subchorionic lake (*) with corresponding feeder vessel at 22 weeks; (d) marginal lake (*) at 20 weeks; and (e) centrolobular lake (*) at 34 weeks, before (left) and after (right) application of gentle probe pressure. AC, amniotic cavity.

the placenta inside the uterine cavity. The higher volume of incoming blood from a larger artery may increase the size of the corresponding centrolobular cavity, creating the image of a lake on ultrasound (Figure 2).

Ultrasound morphology

Placental lakes are the most common placental feature seen on grayscale ultrasound. They are defined at the mid-pregnancy scan as homogeneous anechoic areas of > 2 cm in diameter, surrounded by placental tissue of normal echogenicity^{10–12}. They are often found in the center of a lobule or cotyledon, under the chorionic plate or in the marginal zone (Figure 1) from the end of the first trimester (Figure 2) and often contain turbulent, low-velocity flow. The reported prevalence in the general population varies from 2% to 71%, due to the use of different definitions and gestational ages at examination^{13–16}. Their size, number and shape can also change with maternal position, uterine contractions, location of the placenta inside the uterine cavity and with direct pressure of the ultrasound probe¹⁶ (Figure 1e). Videoclip S1 summarizes the key ultrasound features of placental lakes.

In uncomplicated pregnancies, the development of placental lakes is usually not associated with any changes in the surrounding villous structure on histology³, irrespective of the size of the lake (Figure 3). Marginal lakes and lakes between lobes in a bilobed placenta can be very large (> 5 cm) and are of no clinical significance. By contrast, pregnancies complicated by vasculopathies of the spiral arterioles and placental malperfusion often present with a combination of secondary placental macroscopic lesions, including intervillous and parabasal thrombosis, hematomas, infarcts and extensive fibrin deposition¹⁷.

Changes in the peripheral echogenicity of a lake have been associated with the development of intervillous



Figure 2 Longitudinal transabdominal ultrasound images of placenta (P) in first-trimester uncomplicated pregnancies, showing: (a) intraplacental lake (*) at 12 weeks; and (b) centrolobular lake (*) with corresponding feeder vessels on color Doppler imaging at 13 weeks. AC, amniotic cavity.

thrombosis (Figure 4) and an increase in maternal serum alpha-fetoprotein level secondary to breakdown of the villous barrier^{15,18–21}. The ultrasound features of intervillous thrombosis change with advancing gestation as more fibrin is deposited in the lake periphery and depending on when or if the maternal blood clots in its center^{3,21}. In the most severe cases, there is evidence of abnormal intervillous circulation from the beginning of the second trimester, which is characterized by multiple lakes of variable size and shape and major placental anatomical changes. The placenta may appear thickened on ultrasound, with patchy areas of sonolucencies and an abnormal texture, appearing to ‘wobble’ in an abnormal, ‘jelly-like’ fashion¹⁰ (Figure 3d). These features refer to the overall appearance of the placenta, which has its chorionic plate pushed up by jet-like bloodstreams, with an overall reduction in the echogenicity of the placental mass.

The mechanism that leads to development of an echogenic ring around a centrolobular cavity (Figure 4) is unknown. On histology, these changes correspond to perivillous fibrin deposits forming a shell around the lake, blocking free circulation around the villi and resulting in

macroscopic centrolobular intervillous thrombosis^{3,19–22}. As these lesions are often limited to one lobule, they are rarely associated with a reduction in fetal growth.

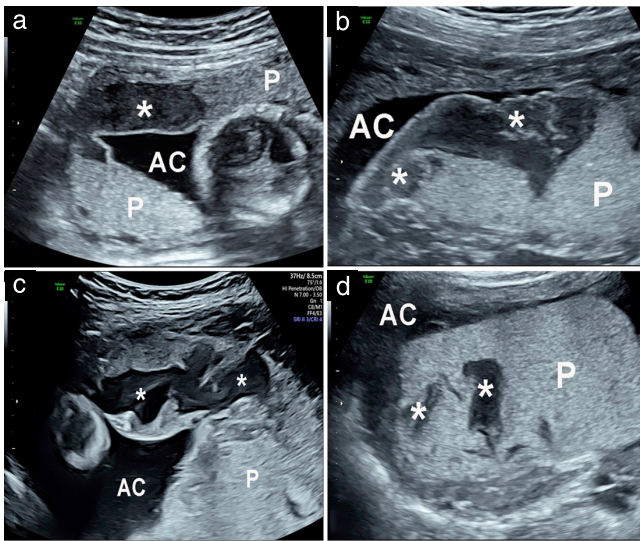


Figure 3 Longitudinal ultrasound images of placentas (P) with large lakes (★). (a) Lake is situated between two lobes in bilobed placenta at 20 weeks. (b) Subchorionic lake is connected to marginal lake at 20 weeks. (c) Lake in upper lobe of bilobed placenta previa at 33 weeks in uncomplicated pregnancy. (d) 'Jelly-like' appearance of entire placenta at 23 weeks in pregnancy complicated by severe intrauterine growth restriction (estimated fetal weight < 5th centile) and increased resistance to blood flow in umbilical and uterine circulation. AC, amniotic cavity.

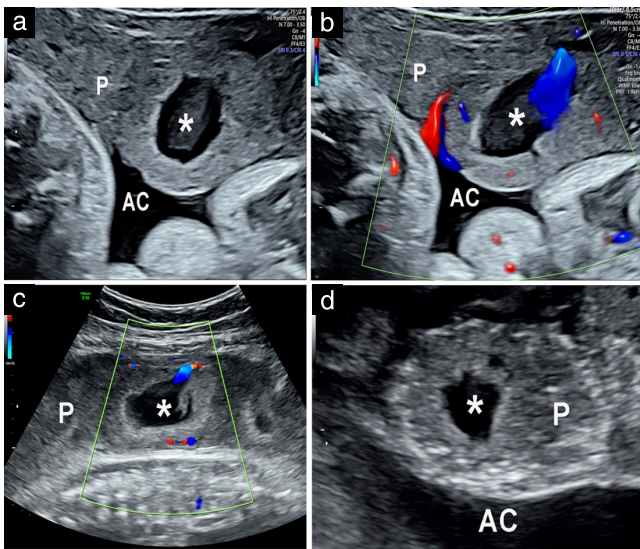


Figure 4 Longitudinal ultrasound images of placentas (P), showing centrolobular lakes (★) with increased peripheral echogenicity (echogenic cystic lesions) that were confirmed at birth to be chronic intervillous thrombosis. (a,b) Pregnancy complicated by intrauterine growth restriction (estimated fetal weight, 8th centile) at 34 weeks; note blood entering lake and corresponding feeder vessel on color Doppler imaging. (c) Uncomplicated pregnancy at 33 weeks (estimated fetal weight, 60th centile); note thick layer of echogenic tissue surrounding lesion and corresponding feeder vessel on color Doppler imaging. (d) Uncomplicated pregnancy at 33 weeks; note increased echogenicity of villous tissue at periphery of corresponding placental cotyledon. AC, amniotic cavity.

Clinical outcomes and prognosis

The occurrence of placental lakes at different time-points during gestation has been associated with malperfusion-related pregnancy complications by several authors. Baldassarre *et al.*¹⁵ reported that the presence of placental lakes of ≥ 0.7 cm in diameter at 11–13 weeks of gestation is associated with higher incidence of placenta previa, marginal sinus (Figure 3b) and subchorionic hemorrhage compared with placental sonolucencies < 0.7 cm, but there was no difference in the rate of adverse obstetric outcome. Similarly, Thompson *et al.*¹¹ and Reis *et al.*¹³ detected no association between the finding of placental lakes during the second or third trimester and uteroplacental complications or adverse pregnancy outcome. By contrast, Kofinas *et al.*²³ reported a higher incidence of pre-eclampsia and intrauterine growth restriction (IUGR) in patients presenting with hypoechoic areas of the placental parenchyma at the mid-pregnancy ultrasound examination. Wan Masliza *et al.*²⁴ also found that placental lakes and increased placental thickness at 20–32 weeks were associated with pre-eclampsia and IUGR.

Echogenic cystic lesions, defined as lesions with a hypoechoic center and a characteristic echogenic halo located inside one or more placental cotyledon(s) (Figure 4), are more likely to be associated with placental malperfusion than are simple lakes. Proctor *et al.*²⁰ found that these lesions are most commonly due to intervillous thrombosis and are associated with severe pre-eclampsia and extreme IUGR in 20% and 18% of cases, respectively. Isolated small intervillous thromboses are of no clinical significance and are commonly found in the placenta of uncomplicated pregnancies¹⁰. Large lakes are commonly found between the lobes of a bilobed placenta (Figure 3a) or near the marginal edge (Figure 3b,c) and are not associated with specific antenatal complications. Massive subchorionic thromboses, also called Breus' mole, may disrupt the umbilical circulation and have been associated with IUGR and stillbirth^{21,26,27}.

Adverse clinical outcomes may be mediated by associated lesions of placental malperfusion, such as basal-plate microinfarcts and massive perivillous fibrin deposits, which are not readily detectable on ultrasound. By contrast, the jelly-like appearance of the whole placenta on ultrasound (Figure 3d) is an indication of extended placental malperfusion and is often associated with pre-eclampsia and early IUGR¹⁰. It has been suggested that jelly-like placenta is associated with a narrow basal plate²⁷ and subsequent abnormal development of the uteroplacental circulation¹⁰. In these cases, histological examination shows diffuse microinfarction of the basal plate and generalized intervillous fibrin deposition, suggesting that the maternal blood enters the intervillous space at a greater velocity than normal²². These jet-like streams surrounded by turbulence push the chorionic plate up, rupturing the anchoring villi, and the altered hemodynamics within the intervillous space result in thrombosis and excessive perivillous fibrin deposition¹⁰, impairing maternofetal exchange¹⁷.

PLACENTAL LACUNAE

Genesis

Placental lacunae are likely to result, in the context of accreta placentation, from progressive distortion of the normal lobular anatomy, including the interlobular septa^{16,28–30}, when the intervillous circulation is established at the end of the first trimester. The vascular changes associated with accreta placentation are progressive and caused by the development of one or more lobules within a uterine scar area^{30,31}. In a large Cesarean scar defect or niche, the normal uterine structure is replaced by a thin layer of scar tissue made of only sparse myofibers embedded in deposits of collagen and fibrin³⁰. Due to the loss of the normal decidual layer and its spiral arteries, in addition to the inner myometrium with its junctional zone and most of the outer myometrium, the remaining myometrial thickness of large niches is often < 2 mm. Consequently, the basal plate of one or more lobule(s) develops next to the large arterial circulation of the uterine periphery (Figure 5) and the intervillous space of the corresponding lobule is fed by radial and/or arcuate arteries.

In normal placentation, the typical flow rate through a normal spiral artery at term has been calculated to be in the order of 0.125 mL/s²². The physiological transformation of the spiral arteries reduces the flow velocity substantially to values in the region of 0.5–1 cm/s at their opening into the intervillous space. Conversely, peak systolic velocities of feeder arteries entering an accreta lobule are often above 30 cm/s^{30,32}.

In the first trimester of a Cesarean scar pregnancy, the high-volume, high-velocity flows from the radial/arcuate

arteries may dislodge the trophoblastic plugs controlling the entry of maternal blood into the intervillous space³⁰. The outcome likely depends on how much of the gestational sac develops inside the niche. The premature entry of a large amount of maternal blood into the entire placental tissue of a Cesarean scar pregnancy will almost certainly lead to miscarriage³³ (Figure 6a); whereas, if limited to one or two lobules, it will lead to their distortion, including the interlobular septum, and alter the venous return with the secondary formation of lacunae on ultrasound imaging^{29,30} (Figure 5).

In an ongoing Cesarean scar pregnancy, lacunae become increasingly prominent and their development is associated with thick fibrinoid deposition at the uteroplacental interface³⁴. These histologic changes are associated with distortion of Nitabuch's membrane and can explain the loss of parts of the physiological site of detachment of the placenta from the uterine wall in placenta accreta spectrum (PAS). Large, recent (fresh) intervillous thromboses in direct contact with the basal plate and extending to at least half of the placental tissue thickness are found at birth in most cases of PAS with six or more lacunae on ultrasound imaging³⁵. There are no microscopic morphological alterations of the villous architecture above the abnormally attached areas^{34–36}.

Ultrasound morphology

Placental lacunae are large, irregular, sonolucent intraplacental spaces often described as giving the placenta a 'moth-eaten' appearance on both transabdominal and transvaginal grayscale ultrasound imaging^{16,37–39}

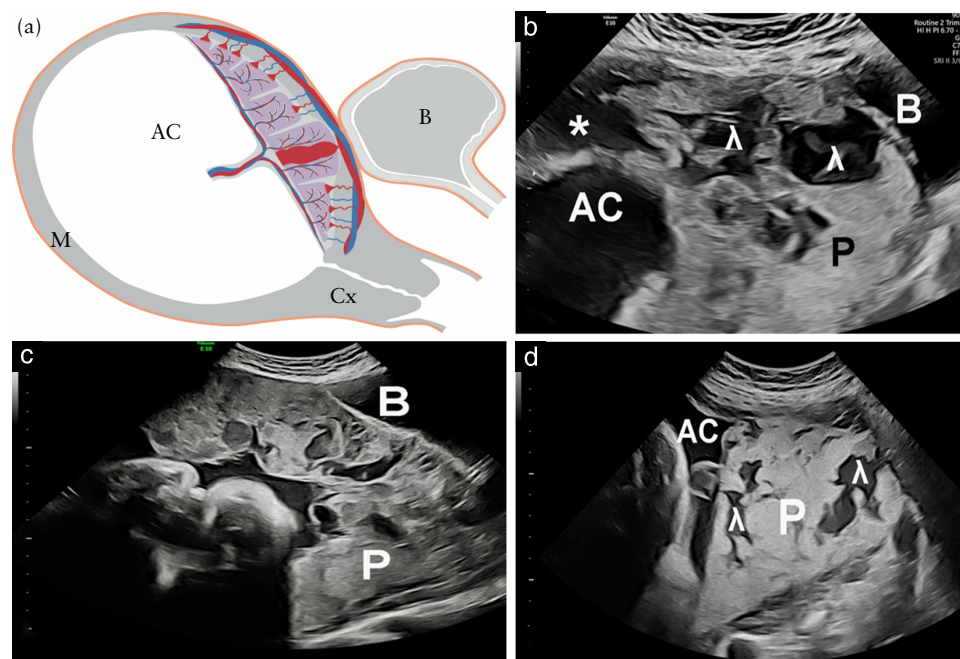


Figure 5 (a) Diagram of placenta previa accreta with lacuna fed directly by radial artery in scar area under bladder (B). (b–d) Longitudinal transabdominal ultrasound images of placenta (P) in pregnancies diagnosed with placenta increta at birth, showing typical moth-eaten appearance of placenta due to multiple lacunae (λ) (ultrasound score, 3+). (b) Multiple lacunae and marginal lake (*) at 25 weeks. (c) Multiple lacunae with increased placental thickness at 32 weeks. (d) Multiple lacunae with lack of clear space and myometrial thinning at 35 weeks. AC, amniotic cavity; Cx, cervix; M, myometrium.

(Figures 5 and 7). The maternal position, uterine contractions and direct pressure of the ultrasound probe are not associated with major changes in the shape or number of lacunae¹⁶. In 1992, Finberg and Williams³⁷ were the first to describe placental lacunae and to propose a classification system based on the number of lacunae. The ultrasound characteristics of lacunae are summarized in Videoclip S1.

As over 95% of PAS cases occur in patients with a prior Cesarean delivery presenting with a low-lying placenta/placenta previa⁴⁰, placental lacunae are found in association with remodeling of the underlying lower uterine segment (LUS) wall following scarring. These anomalies of the uterine contour include chiefly myometrial thinning and loss of the clear zone, of which both can be seen

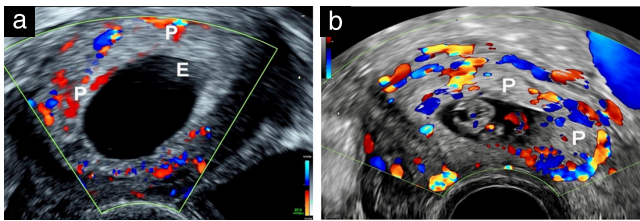


Figure 6 Longitudinal transvaginal ultrasound images with color Doppler mapping of placenta (P) and lower uterine segment. (a) Gestational sac in intrauterine missed miscarriage at 10 weeks (based on last menstrual period (LMP)) containing embryonic (E) remnants. Placental tissue is heterogeneous with multiple small sonolucencies, due to premature entry of maternal blood flow into intervillous space. (b) Gestational sac in Cesarean scar pregnancy at 10 weeks (based on LMP), containing live fetus. Placental tissue is heterogeneous with multiple small sonolucencies and there is increased vascularization around gestational sac.

on grayscale two-dimensional (2D) ultrasound imaging at the mid-pregnancy fetal anatomy scan³⁹. The LUS is much thinner compared with the upper segment and contains fewer myofibers and more elastic connective tissue⁴¹. As pregnancy advances into the third trimester, the progressive stretching of the LUS is associated with further thinning of the residual myometrium in the scar^{42,43}. The dehiscence of the LUS leads to the progressive herniation of the underlying placental tissue towards the bladder, which is described on grayscale 2D ultrasound as the ‘placental bulge’^{42,43}.

In both normal and accreta placentation, placental development in the LUS is often associated with more prominent dilatation of the vasculature on CDI³¹ (Figure 8). As radial arteries account for approximately 90% of the total uteroplacental vascular resistance²², this may not be associated with obvious changes in intervillous circulation until after 16 weeks of gestation³¹. Similarly to anomalies of the uterine contour, anomalies of both the uteroplacental and intervillous circulation will become more prominent on ultrasound imaging as the pregnancy advances into the third trimester^{39,43}. These include, in addition to placental lacunae, an increase in subplacental vascularization and the presence of large feeder vessels connecting the arcuate arteries directly to the lacunae^{16,30,35,43}. The changes are better evaluated on CDI (Figure 9) and allow the differential diagnosis between lacunae associated with PAS and lacuna-shaped sonolucencies (Figure 10).

Maternal bladder filling improves the visualization of placental lacunae and the uteroplacental circulation on transabdominal ultrasound⁴⁴. Transvaginal sonography is essential to confirm the placental position and provide a

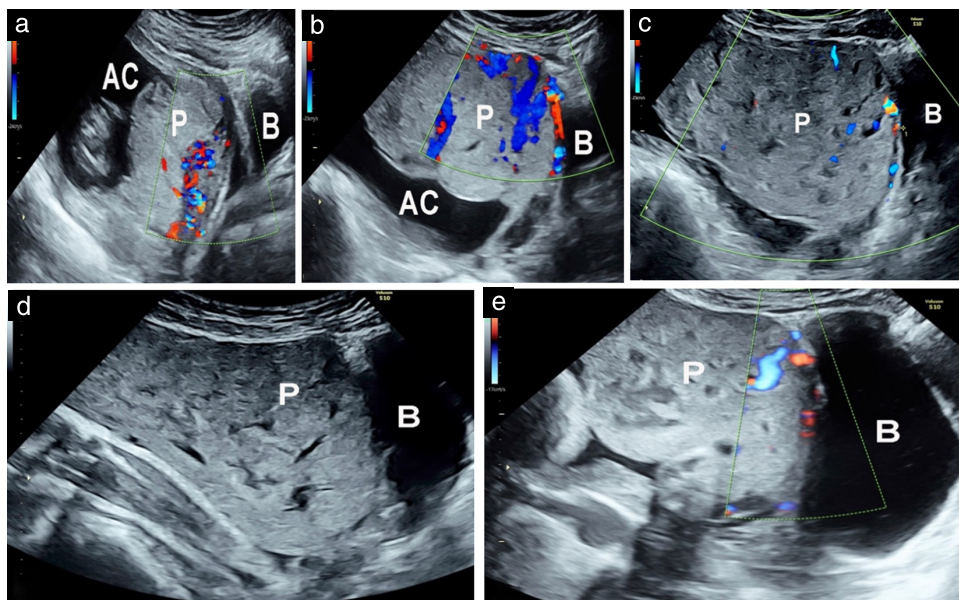


Figure 7 Longitudinal transabdominal ultrasound images of placenta (P) and lower uterine segment in patient with low-lying anterior placenta accreta at birth managed by peripartum hysterectomy, showing progressive development of placental lacunae: (a) no lacunae visible at 12 weeks; (b) lacunae score of 2+ with feeder vessels at 20 weeks; (c) lacunae score of 3+ at 24 weeks; (d) lacunae score of 3+ at 28 weeks; and (e) lacunae score of 3+ with feeder vessels at 34 weeks. Note change in uterine contour (lack of clear space and myometrial thinning) from 20 weeks. AC, amniotic cavity; B, bladder.

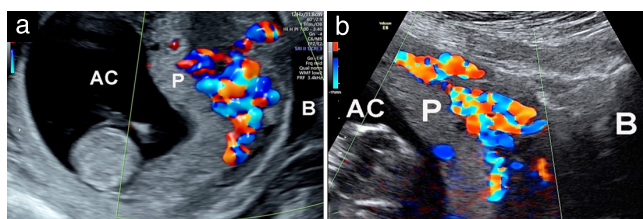


Figure 8 Longitudinal transabdominal ultrasound images with color Doppler of placenta (P) and lower uterine segment in patients with multiple prior Cesarean deliveries, presenting with placenta inserted in lower part of uterine cavity and increased uteroplacental circulation at 11 weeks (a) and at 12 weeks (b). In both cases, placental and uterine structures appear anatomically normal. Both patients had marginal placenta previa with no evidence of placenta accreta spectrum at birth. AC, amniotic cavity; B, bladder.

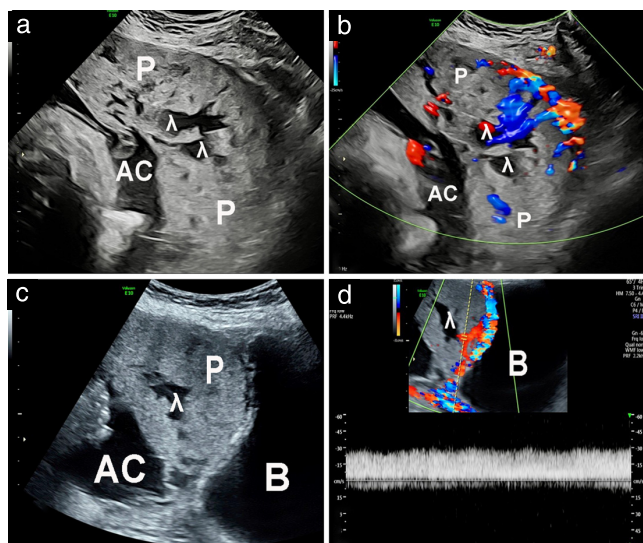


Figure 9 Longitudinal ultrasound images of placenta (P) and lower uterine segment in patients with multiple prior Cesarean deliveries, presenting with marginal placenta previa and diagnosed with placenta previa accreta at birth. (a,b) Numerous lacunae (λ) (score 3+) at 35 weeks; increased subplacental vascularity and feeder vessels are evident on color Doppler imaging. (c,d) Large lacuna (λ) at 28 weeks, with lack of clear space, myometrial thinning and placental bulging; increased subplacental vascularity and feeder vessel with blood flow velocity of ~ 30 cm/s are evident on color Doppler imaging. AC, amniotic cavity; B, bladder.

more accurate evaluation of the anatomy of the LUS and corresponding vascular changes associated with placenta previa accreta, including the development of placental lacunae⁴⁵.

Clinical outcome and prognosis

The presence of placental lacunae in the second half of pregnancy has become synonymous with PAS³⁹, and the number of lacunae is associated with the severity of PAS at birth (Figures 5 and 9) and surgical outcome^{46,47}. Of the 11 standardized ultrasound signs associated with a high probability of PAS at birth, placental lacunae is the only sign to have been quantified successfully³⁹. The method of choice to quantify placental lacunae for 26/37 (70.3%)

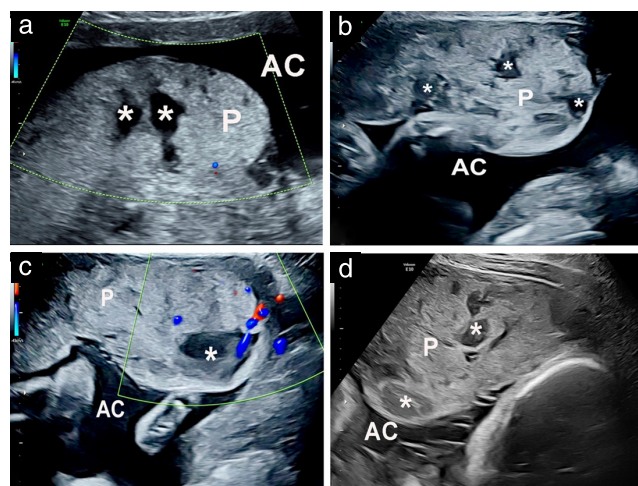


Figure 10 Longitudinal transabdominal ultrasound images of placenta (P) with lacuna-shape sonolucencies (\star) in nulliparous patients with no surgical history. (a) Posterior high placenta with two large pseudolacunae and no increase in uteroplacental circulation at 20 weeks. (b,c) Anterior high placenta with multiple irregular sonolucencies at 20 weeks; color Doppler mapping (c) shows no increase in uteroplacental circulation. (d) Same case as in (b,c) at 32 weeks, with normal fetal growth.

panelists involved in a modified Delphi process is the score proposed by Finberg and Williams³⁷, i.e. none, 0; 1–3, 1+; 4–6, 3+; and > 6 , 3+.

Interestingly, these hemodynamic changes within the intervillous space in accreta placentation do not seem to be associated with damage to the villous tissue surrounding the lacunae^{34–36} or impairment in fetal growth. A large multicenter study found no difference in fetal growth for pregnancies with placenta previa and a PAS disorder compared to those with only placenta previa and those with a low-lying placenta⁴⁸. There was no increased incidence of abnormal fetal growth in cases of placenta previa complicated by PAS compared to those with placenta previa that separated spontaneously at birth.

CASE SERIES

We present ultrasound images and videoclips from 30 patients, including: 10 patients referred for a detailed examination at 20–23 weeks of gestation because of abnormal placental parenchyma in the second half of pregnancy, who had at least one follow-up scan before delivery; 10 patients at high risk of PAS at birth (history of multiple Cesarean deliveries and anterior low-lying placenta) screened at 11–14 weeks of gestation, including five with and five without confirmation of PAS at birth, with follow-up scans at 20–23 weeks, 28–30 weeks and 32–34 weeks; and 10 patients with a high probability of PAS at birth (history of multiple Cesarean deliveries, anterior low-lying placenta or placenta previa⁴⁹ and ultrasound signs suggesting PAS³⁹), referred for surgical planning at 32–36 weeks. All patients underwent detailed transabdominal and transvaginal ultrasound examinations (Voluson E10; GE Medical

Systems, Zipf, Austria), including CDI mapping of the placenta and uteroplacental interface, within 48 h before their planned Cesarean delivery date.

Placental parenchymal lesions visualized on ultrasound were reviewed using standardized descriptors, including size, number, position and association with abnormalities of the uterine contour (lack of clear space, myometrial thinning and placental bulging) and of the uteroplacental circulation. The diagnosis of PAS was confirmed at birth according to intraoperative features and macroscopic examination of hysterectomy specimens with placenta *in situ* or specimens for partial myometrial resection, as described previously³⁶. The score proposed by Finberg and Williams³⁷ was used to record placental lacunae. A detailed histopathologic examination was also performed if the pregnancy was complicated by fetal or maternal complications, as per local protocols.

The main ultrasound findings of the case series are displayed in Table S1. In the subgroup presenting with anomalies of the placental parenchyma at 20–23 weeks, there were two cases of bilobed placenta, two cases with sonolucencies suggestive of lacunae and one case described as jelly-like. At 28–35 weeks, three of the five cases presenting initially with small and large lakes with normal borders had developed echogenic borders, of which one was complicated by IUGR, increased resistance to blood flow in the umbilical circulation and chronic intervillous thrombosis on histopathologic examination. Fetal growth in the case described as jelly-like dropped below the 5th centile at 32 weeks, with increased resistance to blood flow in the umbilical circulation and blood flow redistribution in the fetal middle cerebral artery, and the patient was delivered 48 h after the ultrasound examination. Histopathologic examination identified maternal floor infarction and generalized intervillous fibrin deposition.

In the subgroup of patients at high risk of PAS in whom PAS was confirmed at birth, the number of cases with high lacunae scores (2+ or 3+), uteroplacental hypervascularization and bridging vessels increased with advancing gestation. In all five cases, anomalies of the uterine contour (lack of clear space, myometrial thinning and placental bulging) were found from 20–23 weeks of gestation. Among the five high-risk cases with no evidence of PAS at birth, two had uteroplacental hypervascularization at 11–14 weeks, which was not found on later scans, and two had anomalies of the uterine contour from 28–30 weeks. Placenta previa was noted in seven cases and low-lying placenta in two. All patients referred for surgical planning at 32–36 weeks presented with high lacunae scores (2+ or 3+), uteroplacental hypervascularization and anomalies of the uterine contour, and bridging vessels were found in six cases. Placenta previa and low-lying placenta were observed in nine cases and one case, respectively.

CONCLUSIONS

Knowledge of the pathophysiology and differential diagnosis on ultrasound of different lesions of the placental

parenchyma improves the antenatal care and management of patients presenting with these lesions on routine ultrasound examination. The ultrasound appearance of lakes and lacunae derives from the low echogenicity of villous-free areas within the placental parenchyma, filled with maternal blood of varying velocities. Placental lakes start to appear as soon as the maternal blood begins flowing freely within the intervillous space at the end of the first trimester. Placental lakes, including large ones (> 5 cm), have no clinical significance. Lakes can develop into echogenic cysts, which may be associated with slow fetal growth. Lacunae develop progressively during the second trimester in pregnancies complicated by PAS at birth. In more than 95% of cases, they are found in patients with a history of Cesarean delivery presenting with an anterior low-lying placenta or placenta previa. Lakes and lacunae can coexist in the same placenta and both will change in size and shape as pregnancy advances. What differentiates lacunae from lakes is their association with changes of the underlying uteroplacental circulation and the uterine contour that follows scarring after uterine surgery.

ACKNOWLEDGMENT

We are grateful to Mr David Smithson, Senior Graphic Designer, UCL Digital Media, for his support in making the diagrams.

REFERENCES

1. Tabrisky J, Lindstrom RR, Herman MW, Castagna J, Sarti D. Value of gallbladder B-scan ultrasonography. *Gastroenterology* 1975; **68**: 1246–1252.
2. Spirt BA, Kagan EH, Rozanski RM. Sonolucent areas in the placenta: sonographic and pathologic correlation. *AJR Am J Roentgenol* 1978; **131**: 961–965.
3. Jauniaux E, Campbell S. Ultrasonographic assessment of placental abnormalities. *Am J Obstet Gynecol* 1990; **163**: 1650–1658.
4. Arduini D, Rizzo G, Boccolini MR, Romanini C, Mancuso S. Functional assessment of uteroplacental and fetal circulations by means of color Doppler ultrasonography. *J Ultrasound Med* 1990; **9**: 249–253.
5. Hustin J, Schaaps JP. Echographic and anatomic studies of the materno-trophoblastic border during the first trimester of pregnancy. *Am J Obstet Gynecol* 1987; **157**: 162–168.
6. Foidart JM, Hustin J, Dubois M, Schaaps JP. The human placenta becomes haemochorial at the 13th week of pregnancy. *Int J Dev Biol* 1992; **36**: 451–453.
7. Jauniaux E, Hempstock J, Greenwold N, Burton GJ. Trophoblastic oxidative stress in relation to temporal and regional differences in maternal placental blood flow in normal and abnormal early pregnancies. *Am J Pathol* 2003; **162**: 115–125.
8. Burton GJ, Cindrova-Davies T, Turco MY. Review: Histotrophic nutrition and the placental-endometrial dialogue during human early pregnancy. *Placenta* 2020; **102**: 21–26.
9. Jauniaux E, Jurkovic D, Campbell S, Hustin J. Doppler ultrasonographic features of the developing placental circulation: Correlation with anatomic findings. *Am J Obstet Gynecol* 1992; **166**: 585–587.
10. Jauniaux E, Ramsay B, Campbell S. Ultrasonographic investigation of placental morphologic characteristics and size during the second trimester of pregnancy. *Am J Obstet Gynecol* 1994; **170**: 130–137.
11. Thompson MO, Vines SK, Aquilina J, Wathen NC, Harrington K. Are placental lakes of any clinical significance? *Placenta* 2002; **23**: 685–690.
12. Inubashiri E, Deguchi K, Abe K, Saitou A, Watanabe Y, Akutagawa N, Kuroki K, Sugawara M, Maeda N. Three-dimensional high-definition flow in the diagnosis of placental lakes. *J Med Ultrason* 2014; **41**: 491–494.
13. Reis NS, Brizot ML, Schultz R, Nomura RM, Zugaib M. Placental lakes on sonographic examination: correlation with obstetric outcome and pathologic findings. *J Clin Ultrasound* 2005; **33**: 67–71.
14. Cooley SM, Donnelly JC, Walsh T, McMahon C, Gillan J, Geary MP. The impact of ultrasonographic placental architecture on antenatal course, labor and delivery in a low-risk primigravid population. *J Matern Fetal Neonatal Med* 2011; **24**: 493–497.
15. Baldassarre RL, Gabe M, Pretorius DH, Ramos GA, Romine LE, Hull AD, Ballas J, Pettit KE. Placental sonolucencies in the first trimester: incidence and clinical significance. *Ultrasound Q* 2016; **32**: 43–46.
16. Jauniaux E, Collins SL, Burton GJ. Placenta accreta spectrum: Pathophysiology and evidence-based anatomy for prenatal ultrasound imaging. *Am J Obstet Gynecol* 2019; **218**: 75–87.

17. Burton GJ, Jauniaux E. Pathophysiology of placental-derived fetal growth restriction. *Am J Obstet Gynecol* 2018; **218**: S745–S761.
18. Jauniaux E, Nicolaides KH. Placental lakes, absent umbilical artery diastolic flow and poor fetal growth in early pregnancy. *Ultrasound Obstet Gynecol* 1996; **7**: 141–144.
19. Jauniaux E, Gibb D, Moscoso G, Campbell S. Ultrasonographic diagnosis of a large placental intervillous thrombosis associated with elevated maternal serum alpha-fetoprotein level. *Am J Obstet Gynecol* 1990; **163**: 1558–1560.
20. Proctor LK, Whittle WL, Keating S, Viero S, Kingdom JC. Pathologic basis of echogenic cystic lesions in the human placenta: role of ultrasound-guided wire localization. *Placenta* 2010; **31**: 1111–1115.
21. Prins JM, Sebire N, Khalil A, Gordijn SJ. Imaging of placental pathology. In *Benirschke's Pathology of the Human Placenta*, (7th edn), Baergen RN, Burton GJ, Kaplan CG (eds). Springer, New York, NY, 2022; 869–886.
22. Burton GJ, Woods AW, Jauniaux E, Kingdom JC. Rheological and physiological consequences of conversion of the maternal spiral arteries for uteroplacental blood flow during human pregnancy. *Placenta* 2009; **30**: 473–482.
23. Kofinas A, Kofinas G, Sutija V. The role of second trimester ultrasound in the diagnosis of placental hypoechoic lesions leading to poor pregnancy outcome. *J Matern Fetal Neonatal Med* 2007; **20**: 859–866.
24. Wan Masliza WD, Bajuri MY, Hassan MR, Naim NM, Shuhaila A, Das S. Sonographically abnormal placenta: an association with an increased risk poor pregnancy outcomes. *Clin Ter* 2017; **168**: e283–289.
25. Fox H, Sebire N. *Pathology of the Placenta* (3rd edn). Elsevier, 2007.
26. Alanjari A, Wright E, Keating S, Ryan G, Kingdom J. Prenatal diagnosis, clinical outcomes, and associated pathology in pregnancies complicated by massive subchorionic thrombohematoma (Breus' mole). *Prenat Diagn* 2013; **33**: 973–978.
27. Suri S, Muttukrishna S, Jauniaux E. 2D-Ultrasound and endocrinologic evaluation of placentation in early pregnancy and its relationship to fetal birthweight in normal pregnancies and pre-eclampsia. *Placenta* 2013; **34**: 745–750.
28. Fox H. Placenta accreta: 1945–1969. *Obstet Gynecol Survey* 1972; **27**: 475–490.
29. Jauniaux E, Burton GJ. Pathophysiology of placenta accreta spectrum disorders: A review of current findings. *Clin Obstet Gynecol* 2018; **61**: 743–754.
30. Jauniaux E, Jurkovic D, Hussein AM, Burton GJ. New insights into the etiopathology of placenta accreta spectrum. *Am J Obstet Gynecol* 2022; **227**: 384–391.
31. Jauniaux E, Zosmer N, De Braud LV, Ashoor G, Ross J, Jurkovic D. Development of the utero-placental circulation in cesarean scar pregnancies: a case-control study. *Am J Obstet Gynecol* 2022; **226**: 399.e1–10.
32. Zhang J, Li H, Wang F, Qin H, Qin Q. Prenatal Diagnosis of Abnormal Invasive Placenta by Ultrasound: Measurement of highest peak systolic velocity of subplacental blood flow. *Ultrasound Med Biol* 2018; **44**: 1672–1678.
33. Jauniaux E, Mavrelou D, De Braud LV, Dooley W, Knez J, Jurkovic D. Impact of location in live tubal and cesarean scar ectopic pregnancies. *Placenta* 2021; **108**: 109–113.
34. Jauniaux E, Hussein AM, Elbarmelgy RM, Elbarmelgy RA, Burton GJ. Failure of placental detachment in accreta placentation is associated with excessive fibrinoid deposition at the utero-placental interface. *Am J Obstet Gynecol* 2022; **226**: 243.e1–10.
35. Jauniaux E, Zosmer N, Subramanian D, Shaikh H, Burton GJ. Ultrasound-histopathologic features of the utero-placental interface in placenta accreta spectrum. *Placenta* 2020; **97**: 58–64.
36. Jauniaux E, Hussein AM, Zosmer N, Elbarmelgy RM, Elbarmelgy RA, Shaikh H, Burton GJ. A new methodologic approach for clinico-pathologic correlations in invasive placenta previa accreta. *Am J Obstet Gynecol* 2020; **222**: 379.e1–11.
37. Finberg HJ, Williams JW. Placenta accreta: prospective sonographic diagnosis in patients with placenta previa and prior cesarean section. *J Ultrasound Med* 1992; **11**: 333–343.
38. Jauniaux E, Collins SL, Jurkovic D, Burton GJ. Accreta placentation: a systematic review of prenatal ultrasound imaging and grading of villous invasiveness. *Am J Obstet Gynecol* 2016; **215**: 712–721.
39. Jauniaux E, D'Antonio F, Bhide A, Prefumo F, Silver RM, Hussein AM, Shaikher SA, Chantraine F, Alfirevic Z, Delphi consensus expert panel. Modified Delphi study of ultrasound signs associated with placenta accreta spectrum. *Ultrasound Obstet Gynecol* 2023; **61**: 518–525.
40. Jauniaux E, Chantraine F, Silver RM, Langhoff-Roos J; FIGO Placenta accreta diagnosis and management Expert Consensus Panel. FIGO consensus guidelines on placenta accreta spectrum disorders: Epidemiology. *Int J Gynaecol Obstet* 2018; **140**: 265–273.
41. Schwalm H, Dubrauszy V. The structure of the musculature of the human uterus muscles and connective tissue. *Am J Obstet Gynecol* 1966; **94**: 391–404.
42. Hussein AM, Elbarmelgy RA, Elbarmelgy RM, Thabet MM, Jauniaux E. Prospective evaluation of impact of post-Cesarean section uterine scarring in perinatal diagnosis of placenta accreta spectrum disorder. *Ultrasound Obstet Gynecol* 2022; **59**: 474–482.
43. Jauniaux E, Hussein AM, Einerson BD, Silver RM. Debunking 20th century myths and legends about the diagnosis of placenta accreta spectrum. *Ultrasound Obstet Gynecol* 2022; **59**: 417–423.
44. Maynard H, Zamudio S, Jauniaux E, Collins SL. The importance of bladder volume in the ultrasound diagnosis of placenta accreta spectrum disorders. *Int J Gynaecol Obstet* 2018; **140**: 332–337.
45. Jauniaux E, Hussein AM, Thabet MM, Elbarmelgy RM, Elbarmelgy RA, Jurkovic D. The role of transvaginal ultrasound in the third-trimester evaluation of patients at high risk of placenta accreta spectrum at birth. *Am J Obstet Gynecol* 2023; **229**: 445.e1–11.
46. Hussein AM, Fox K, Bhide A, Elbarmelgy RA, Elbarmelgy RM, Thabet MM, Jauniaux E. The impact of preoperative ultrasound and intraoperative findings on surgical outcomes in patients at high risk of placenta accreta spectrum. *BJOG* 2023; **130**: 42–50.
47. Bhide A, Hussein AM, Elbarmelgy RM, Elbarmelgy RA, Thabet MM, Jauniaux E. Assessment of ultrasound features of placenta accreta spectrum in women at high risk: association with outcome and interobserver concordance. *Ultrasound Obstet Gynecol* 2023; **62**: 137–142.
48. Jauniaux E, Dimitrova I, Kenyon N, Mhallem M, Kametas NA, Zosmer N, Hubinont C, Nicolaides KH, Collins SL. Impact of placenta previa with placenta accreta spectrum disorder on fetal growth. *Ultrasound Obstet Gynecol* 2019; **54**: 643–649.
49. Reddy UM, Abuhamad AZ, Levine D, Saade GR; Fetal Imaging Workshop Invited Participants. Fetal imaging: executive summary of a joint Eunice Kennedy Shriver National Institute of Child Health and Human Development, Society for Maternal–Fetal Medicine, American Institute of Ultrasound in Medicine, American College of Obstetricians and Gynecologists, American College of Radiology, Society for Pediatric Radiology, and Society of Radiologists in Ultrasound Fetal Imaging Workshop. *J Ultrasound Med* 2014; **33**: 745–757.

SUPPORTING INFORMATION ON THE INTERNET

The following supporting information may be found in the online version of this article:

 **Videoclip S1** Video contrasting ultrasound characteristics of placental lakes and lacunae.

 **Table S1** Main ultrasound findings of cases included in study